CFD Letters

SEMARAK ILMU PUBLISHING

Journal homepage:
https://semarakilmu.com.my/journals/index.php/CFD_Letters/index
ISSN: 2180-1363

Thermosolutal Convection of Natural and Anti-Natural Solutions Through an Angled Cavity Under Cross Gradients in Temperature and Concentration

Abdelhakim Mebrouki[1], Redha Rebhi[2,3], Mokdad Hayawi Rahman[4], Giulio Lorenzini[5,*], Younes Menni[6], Houari Ameur[6], Hijaz Ahmad[7]

[1] Mechanical Department, Technology Faculty, University Batna 2, Batna, Algeria
[2] Department of Mechanical Engineering, Faculty of Technology, University of Medea, Medea 26000, Algeria
[3] LERM - Renewable Energy and Materials Laboratory, University of Medea, Medea 26000, Algeria
[4] Aeronautical Technical Engineering, Al-Farahidi University, Baghdad 10011, Iraq
[5] Department of Engineering and Architecture, University of Parma, Parco Area delle Scienze, 181/A, 43124 Parma, Italy
[6] Department of Technology, University Center Salhi Ahmed Naama (Ctr. Univ. Naama), P.O. Box 66, Naama 45000, Algeria
[7] Section of Mathematics, International Telematic University Uninettuno, Corso Vittorio Emanuele II, 39, 00186 Roma, Italy

ARTICLE INFO

Article history:
Received 5 October 2022
Received in revised form 6 November 2022
Accepted 7 December 2022
Available online 1 May 2023

Keywords:
Natural and anti-natural solutions; thermosolutal convection; inclined cavity; concentration gradients; temperature gradients; numerical survey

ABSTRACT

In the current study, cross-temperature and concentration gradients are used to model the *double diffusive natural convection flow* in a binary fluid contained in an angled square cavity. Using a *finite − difference* method, the *mass*, *momentum*, and *energy* conservation equations were numerically solved. The 45° inclined cavity under equal solutal buoyancy and thermal forces was the subject of the study ($N = 1$). Since the horizontal components of the thermal and singular volume forces were equal but opposed to one another, an equilibrium solution for this situation that corresponds to the rest state of the immobile fluid is feasible. However, this equilibrium solution becomes unstable above a specific critical value of the *Rayleigh number*, leading to vertical density stratification inside the enclosure. The results are shown using the *averaged Nusselt* and *Sherwood numbers* as well as the *thermal Rayleigh* and *Lewis numbers* for the flow intensity. The existence of the commencement of convection is demonstrated in this work, and both natural and anti-natural flow solutions are obtained. Subcritical convection has also been seen for the natural solution when the *Lewis number* is more or less than unity. For the start of supercritical and subcritical convection, the *thermal Rayleigh* number's critical values are identified. As the *Rayleigh number* climbed, so did the flow's intensity and the rates at which heat and mass were transferred. Reducing flow intensity and accelerating mass transfer are the results of raising the *Lewis number*. Different flow patterns are shown for an aspect ratio of 4, and the existence interval of the oscillatory solutions is calculated.

* *Corresponding author.*
E-mail address: giulio.lorenzini@unipr.it (Giulio Lorenzini)

https://doi.org/10.37934/cfdl.15.5.97119

1. Introduction

The studies of the natural convective thermal transfer and the double-diffusive natural convective (DDNC) thermal and mass exchange inside a porous medium enclosure have been the subject of an extensive number of experimental, analytical and numerical investigations during the last years using different models. Recently, the conjugate heat transfer phenomena in porous cavities have received a special attention due to their practical importance such as separators in the petroleum field, during the creation of the underground crude, during the storage of radioactive waste, when storing liquid gases, seawater desalination operations, crystal growth, during phase change mechanisms of metals when the micrographic structure and the mechanical and thermo-physical properties of alloys affected directly by convection, and so on [1-4].

Combined buoyancy driven flows due to both temperature and concentration variations in inclined cavities, which tend to be more complex, have not been investigated extensively as the vertical porous medium enclosures, therefore more researches are needed for studying the inclined porous cavities. In the last decade, most research studies into this area have been achieved with the theoretical approach [5-10].

Benhadji and Vasseur [11] compared their numerical and analytical analyses for DDC (double-diffusive convection) of non-Newtonian type fluid saturated a shallow porous cavity, where the power-law model is used to describe the new Newtonian behavior. Bahloul *et al.,* [12] offered a comparison between numerical and analytical linear stability analysis of a binary Newtonian fluid saturated horizontal porous layer with DDC. The outcomes of the analytical and numerical analyses were quite similar. Another article by Bahloul *et al.,* [13] that examined the Soret-induced convection of a Newtonian binary mixture under the influence of cross heat fluxes saturated a horizontal porous type channel. The results demonstrated that the separation parameter and Le (Lewis number) have a role in the migration through subcritical bifurcations for both numerical and analytical study. The rest state stability of Dupuit-Darcy natural convection of a binary fluid saturated vertical porous layer was examined by Rebhi *et al.,* [14] using numerical and analytical analysis. Their primary discovery was that the from drag effect, which serves as a stabilizing impact, considerably affects Hopf bifurcation and subcritical convection. Linear instability and nonlinear stability were used by Kumar *et al.,* [15] to analyze the double-diffusive instability in an inclined porous layer with and without an internal heat source dependent on concentration. The Papanastasiou model for explaining the rheological behavior, Saxena *et al.*, [16], and the lattice Boltzmann method were used to simulate a 2D DDNC. He discovered that an increase in porosity strengthens heat and mass transmission and gradually weakens the unyielded section for a fixed value of the Da (Darcy number). The double-diffusive free convection of a power-law non-Newtonian fluid filled in a horizontal rectangular container was explored analytically and numerically by Bihiche *et al.,* [17]. There were multiple steady state solutions obtained, and there was also good agreement between the numerical and analytical results.

In a square porous type cavity that is isothermally heated from below and cooled from the top and whose vertical boundaries are subject to a horizontal solutal gradient, Bourich *et al.,* [18] researched the thermosolutal convection. To ascertain the specifics of heat and mass exchange in limit instances corresponding to thermal or solutal driven flows, they carried out an analysis based on the scaling law technique. In a thin, vertical, porous hollow that is salted on the sides and heated from below, Bahloul *et al.*, [19] did an analytical assessment for stowing the DDNC. Their findings demonstrated that the solution takes the shape of a typical Bénard bifurcation in the absence of a horizontal solutal gradient $(N = 0)$. Bourich *et al.*, [20] investigated the situation in which a porous enclosure is partially heated from below while being continuously cooled at the top. There is a horizontal concentration gradient applied to the porous matrix's vertical walls. They investigated how the various steady solutions were affected by the solutal buoyancy forces. Their results demonstrated an asymmetric bicellular flow at a predetermined vertical border of the heated side ($\delta = 0.5$). Additionally, they stated that at threshold values of N, the solutal buoyancy forces brought on by horizontal concentration gradients may eliminate the numerous solutions provided by pure thermal convection. According to research by Kramer *et al.,* [21], distinct flow regimes were observed for various values of the governing parameters for DDNC in an enclosure exposed to cross GsCT (gradients of concentration and temperature). Chamkha *et al.*, [22] looked into the scenario of a binary fluid mixture flowing laminarly thermo-solutally in a porous enclosure that was inclined. The cavity's two opposing surfaces are subjected to mixed fluxes of heat and mass along with conditions of uniform T and concentration. They observed a decrease in Sherwood and Nusselt numbers with an increase in the enclosure tilting angle. They noticed a decline in $Sherwood$ and $Nusselt$ values as the tilt of the enclosure increased.

Balla and Naikoti [23] looked at the effects of α angle of cavity inclination, Soret effects, and Dufour impacts on the DDNC in a square type cavity. Heat is delivered to the cavity's two horizontal surface, and solute transverse gradients are used. It was found that when the α increased, the thermal fields significantly changed and the flows adopted vertical patterns rather than horizontal ones. In a 3D porous type enclosure subjected to cross GsCT, Ouzaouit *et al.*, [24] observed thermosolutal convection. Balla *et al.*, [25] used numerical analysis to investigate the effects of the cavity's inclination angle on the flow in the case of the magnetohydrodynamic natural convection of a porous saturated medium supplied with nanofluid in a square type cavity. The same author re-examined the same issue. Balla *et al.*, [26] used the Darcy model to study the magneto-hydrodynamic convection inside a cavity supplied with a flow of nanofluid and affected by viscous dissipation, with the resulting equation being solved using the finite element. DDC having cross variations on heat and mass transmission in a cubical type enclosure including adiabatic cylinder type obstacles was statistically investigated by Chakkingal *et al.*, [27]. Rebhi *et al.*, [28] looked at how inertial forces affected convection in an angled square type cavity under the influence of a magnetic field. According to a study by Ouazaa *et al.*, [29] of DDNC in a cavity of square type with an angled permeable medium exposed to cross GsCT, an equilibrium solution relating to the rest state is possible for the case where the buoyancy forces are equal and the inclination angle is $45°$, and the resulting onset of motion can be either supercritical or subcritical.

Based on the Buongiorno's mathematical model, Ghiasi and Saleh [30], their key conclusion is that viscous dissipation and the resistive Lorentz force have a significant impact on the thermal boundary layer thickness. Khdher *et al.,* [31] explored the case of a secondary flow inside a square, straight type duct using H_2O as the base fluid and three different kinds of nanofluids (Al_2O_3, TiO_2, and CuO) with constant heat flux in the top and bottom surfaces. The nanofluid containing CuO nanoparticles had the greatest Nu number in their investigation, followed by TiO_2 and Al_2O_3, respectively. Khan *et al.,* [32] demonstrated that, for a vertical permeable sheet, the lowered coefficient of friction, and local $Nusselt$ value rise with rising heat source parameters as well as chemical reaction and characteristics. Yusof *at al.,* [33] examined the steady Casson fluid flow at the stagnation point and radiative transfer of heat as it crossed a slippery, exponentially porous Riga plate. In a porous media with the presence of heat radiation and viscous dissipation, Wahid *et al.,* [34] explored analytically the magnetohydrodynamic slip Darcy flow of viscoelastic fluid across a stretching surface. Mahrous *et al.,* [35] went over how the CFD models of cerebral aneurysms differed between non-Newtonian and Newtonian modeling methodologies. They noticed that the non-Newtonian model could most accurately depict blood flow in an intracranial aneurysm. Other similar studies are cited in these referenced numericals simulations [36,37].

Paliwal and Chen [38,39] investigated the impact of a fluid layer's inclination on the threshold of thermosolutal convection. In this problem, they imposed an initial solutal stratification in the vertical direction and then a lateral heating was used on the cavity's vertical walls. In the first part, an experimental study was carried out by altering the angle of inclination that is taken into account in relation to the horizontal plane through a range of angles of inclination ($-75°$ to $+75°$: a negative angle indicates a heating of the upper wall and a positive angle denotes heating of the lower wall), the results demonstrated the periodic formation of convective cells whose structure and regime strongly depend on the angle of inclination of the system. Regarding the critical thermal Rayleigh number, the results showed that they are non-symmetrical with respect to the horizontal state ($\theta = 0°$); heating the bottom wall is more stable than heating the top wall.

Recently, Bodduna *et al.*, [40] studied numerically the activation energy process in biconvection nanofluid flow through porous cavity. The Darcy model was applied to model the convection flow. Also, the Pedley and Kessler model is utilized for the concentration equations of gyrotactic microorganisms. It was demonstrated that the Peclet number and activation energy show a destabilizing effect on the iso-concentrations of nanoparticle volume fraction and microorganisms. The DDC on the peristaltic flow of hyperbolic tangent nanofluid inside a non-uniform type duct with generated magnetic field was investigated by Akram *et al.*, [41] using numerical and analytical methods. The impact of volume fraction of nanoparticles, axial induced magnetic field, magnetic force function on the concentration, temperature, stream function, pressure rise and pressure gradient was presented. With six constant Jeffreys acting, as the base fluid, through an asymmetric type duct, Saeed *et al.*, [42] looked into the theoretical impact of slip barriers on the double diffusion over the peristaltic flow of a nanofluid. By considering the impact of nanomaterial effects on magnetic field induction and DDC on the peristaltic flow of $Prandtl$ nanofluids in an inclined asymmetric type duct, Akram *et al.*, [43] re-examined the same issue. Phu and Thao [44] looked into the effect of Re and inclination angle in the flat tube on the thermos-hydraulic performance. Using the Carreau-Yasuda model to simulate the rheological behavior of a non-Newtonian fluid, Lounis *et al.,* [45] examined the impacts of the Dufour and Soret effects on a DDC inside an angled square type enclosure. Their primary discovery was that the $Lewis$ number boosts heat and mass exchange for various power-law index values.

The study of Mebrouki *et al.*, [46], in which the authors investigated the DDNC flow in a binary fluid enclosed in a slanted square type enclosure susceptible to cross solute and heat fluxes, served as the inspiration for the current investigation. The authors demonstrated through numerical analysis that when the $Lewis$ number was greater or less than unity, the commencement of motion from the rest state was subcritical. Additionally, they showed that there are numerous solutions, both natural and anti-natural, for a certain set of governing factors. The same issue has been looked at for the situation when the thermal and solutal buoyancy forces are equal ($N = 1$) and competing with one another in order to support their findings. To the best of the authors' knowledge, comprehensive research into the impact of cross-fluxed heat and solute on the rates of heat and mass transfer within a slanted square type cavity has not yet been done. The current study demonstrates the presence of multiple solutions for the case where the buoyancy forces are equal ($N = 1$) by showing that two steady-state solutions, i.e., natural and anti-natural, coexist for the same governing parameters. Furthermore, a relationship between the $Lewis$ number and the threshold of convective instability is shown. The formulation of the issue and the numerical approach utilized to resolve the full set of nonlinear governing equations are covered in the next section. The results are addressed as a function of the governing parameters and are provided in terms of $stream\ function$, $temperature\ profiles$, and $heat\ transfer$. Some final thoughts are contained in the last section.

2. Mathematical Details

The case study is an inclined square cavity, as shown in Figure 1 [46]. The fluid being employed is a binary mixture, considered Newtonian. Two of the cavity's parallel walls were mass impermeable subject to regular heat fluxes, q', while the other two walls were adiabatic and susceptible to constant mass fluxes, j'.

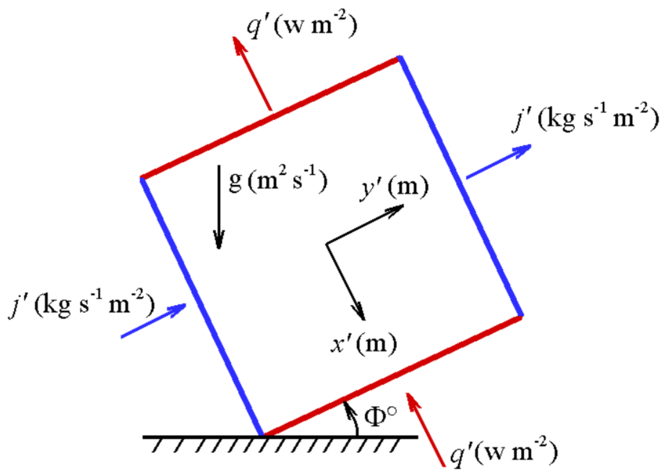

Fig. 1. Geometry and coordinates system for flow setup

Under the previous assumptions, the equations governing the double-diffusive convection are detailed below (continuity, momentum, energy and solute concentration conservation equations). They are given in dimensionless form using a stream function-vorticity (ψ, ω) formulation (see for instance, Paliwal and Chen [39], Mamou *et al.*, [47] and Lee and Hyun [48]):

$$\frac{\partial \nabla^2 \psi}{\partial t} - \frac{\partial \psi}{\partial x}\frac{\partial \nabla^2 \psi}{\partial y} + \frac{\partial \psi}{\partial y}\frac{\partial \nabla^2 \psi}{\partial x} = Pr \nabla^4 \psi - Pr\ Ra_T \left(\sin\Phi \frac{\partial (T+N\,S)}{\partial x} + \cos\Phi \frac{\partial (T+N\,S)}{\partial y} \right) \tag{1}$$

$$\nabla^2 \psi = -\omega \tag{2}$$

$$\nabla^2 T = \frac{\partial T}{\partial t} - \frac{\partial \psi}{\partial x}\frac{\partial T}{\partial y} + \frac{\partial \psi}{\partial y}\frac{\partial T}{\partial x} \tag{3}$$

$$\nabla^2 S = Le\left(\frac{\partial S}{\partial t} - \frac{\partial \psi}{\partial x}\frac{\partial S}{\partial y} + \frac{\partial \psi}{\partial y}\frac{\partial S}{\partial x} \right) \tag{4}$$

$$u = \frac{\partial \psi}{\partial y}\ ; \quad v = -\frac{\partial \psi}{\partial x} \tag{5}$$

Where,
Ra_T: the $thermal\ Rayleigh$,
Pr: the $Prandtl\ number$, and
Le: the $Lewis\ number$.

These are the corresponding dimensionless conditions to the limits (see for example, Paliwal and Chen [39], Mamou *et al.*, [47] and Lee and Hyun [48]):

$$\left.\begin{array}{llll} y = \pm\frac{1}{2} & \psi = \frac{\partial \psi}{\partial x} = 0, & \frac{\partial T}{\partial y} = 0 & \frac{\partial S}{\partial y} = -1 \\ x = \pm\frac{1}{2} & \psi = \frac{\partial \psi}{\partial y} = 0, & \frac{\partial T}{\partial x} = 1 & \frac{\partial S}{\partial x} = 0 \end{array}\right\} \tag{6}$$

Where,
ω: the $dimensionless\ vorticity$,
ψ: the $stream\ function$,
T: the $temperature$, and
S: the $solute\ concentration.$

The $average\ Nusselt$ equation describing the thermal exchange rate is as follows:

$$Nu_m = \int_{-\frac{1}{2}}^{+\frac{1}{2}} \frac{1}{T_{\left(\frac{1}{2},y\right)} - T_{\left(-\frac{1}{2},y\right)}} dy \tag{7}$$

As measured by the rate of mass exchange, the $Sherwood\ number$ is given by:

$$Sh_m = \int_{-\frac{1}{2}}^{+\frac{1}{2}} \frac{1}{S_{\left(x,-\frac{1}{2}\right)} - S_{\left(x,\frac{1}{2}\right)}} dx \tag{8}$$

3. Computational Solution

The SFD approach ($second - Order\ Finite - Difference$) with uniform grids was used to arrive at the numerical solution of the complete governing equations. A $time - accurate$ technique based on the ADI method ($Alternating\ Direction\ Implicit$) was used to solve the $discretized\ vorticity$ (Eq. (1)), $energy$ (Eq. (3)) and $concentration$ (Eq. (4)).

Using the SOR method ($Successive - Over - Relaxation$) and known temperature and concentration distributions, the $stream\ function$ (Eq. (2)) was solved. The temporal terms included in the governing equations were discretized using a FOBFD approach ($First - Order\ Backward\ Finite\ Difference$). LLT method ($Line - by - line\ iterative$) was used to solve the algebraic equations.

The approach used a TMI ($Tri - diagonal\ Matrix\ Inversion$) to solve the system of equations that was produced by sweeping the integrated domain along the axes, X and Y.

The SOR method's convergence requirement was taken into account, $\sum\left|\left(\psi_{i,j}^{k+1} - \psi_{i,j}^{k}\right)\right| / \sum\left|\left(\psi_{i,j}^{k+1}\right)\right| \leq 10^{-6}$, with k denoting the kth iteration and i, j denoting the position of the grid node.

Any further lowering of the criterion of the convergence below 10^{-6} was found to have no discernible impact on the outcomes. For the majority of the examples investigated in this study, the grid size of 81×81 was chosen, with the time step Δt varying from 10^{-4} to 10^{-3}, which provides a suitable compromise between the execution time and the calculation accuracy; may be seen in the determined analytical solution and the numerical findings, as presented in Table 1.

Table 1
Grid sensitivity study for Ra_T =10^5 and Le = 1

$N_x \times N_y$	21 × 21	41 × 41	61 × 61	81 × 81	101 × 101	121 × 121
ψ_0	11.456	11.336	11.288	11.272	11.273	11.275
Nu_m	4.274	4.238	4.209	4.198	4.198	4.198
Sh_m	3.684	3.614	3.593	3.574	3.575	3.575

The validation of the numerical technique was conducted for natural convection phenomenon in a square enclosure against the results of Davis [2] for $A = 1$, $Pr = 0.71$, $Le = 1$ and $N = 0$, and Mamou *et al.*, [47] for $A = 1$, $Ra_T = 10^6$, $Pr = 7.0$, $Le = 10$ and $N = 1$ as demonstrated in Table 2 and Table 3.

Table 2
Comparing the Ψ_0 and Nu_m using some formerly examined numerical findings for $A = 1, Pr = 0.71$, $Le = 1$, $N = 0$ and various values of Ra_T

	Ψ_0			Nu_m		
Ra_T	Davis [2]	Current analysis	Current analysis vs. Davis [2] (%)	Davis [2]	Current analysis	Present analysis vs. Davis [2] (%)
10^3	1.174	1.174	0.00	1.118	1.118	0.00
10^4	5.071	5.069	3.94×10^{-2}	2.243	2.248	2.22×10^{-1}
10^5	9.111	9.104	7.68×10^{-2}	4.519	4.549	6.63×10^{-1}

Table 3
Comparing the Ψ_0, Nu_m, Sh_m, ΔT_{max} and ΔS_{max} with a few previously researched numerical results for $A = 1, Ra_T = 10^6$, $Pr = 7.0, Le = 10$ and $N = 1$

	Mamou *et al.*, [47]	Current analysis	Current analysis vs. Mamou *et al.*, [47] (%)
Ψ_0	6.268	6.261	1.11×10^{-1}
Nu_m	6.536	6.539	4.58×10^{-2}
Sh_m	15.318	15.377	2.01×10^{-1}
ΔT_{max}	0.440	0.438	4.55×10^{-1}
ΔS_{max}	0.185	0.181	2.18×10^{0}

4. Findings and Analysis

The case of the enclosure tilt angle $\Phi = 45°$ and $N = 1$ was considered in this survey. The impact of the Ra and Le on the hydrodynamic and thermal and mass exchange rates were investigated. The situation corresponding to $N = 1$ and $\Phi = 45°$ could result in stable motionless state, which became instable above certain critical Rayleigh numbers. In the motionless state, there was a vertical density stratification within the enclosure due to the same magnitude of solutal and thermal forces but in opposite directions. This situation was studied experimentally and theoretically in the past by Paliwal and Chen [38,39] in a tilted slender fluid layer. Overall, there was a supercritical Rayleigh number for the occurrence of convection, below which subcritical convection existed when thermal and solutal diffusivities were not equal ($Le \neq 1$). Obviously, the thresholds for the occurrence of supercritical or subcritical convection depended on the Le number. For moderate Le values of, the natural and anti-natural solutions of convection coexist.

The natural solution was defined for the fact that it prevails during the initiation of convection from a still state. When the Le number was greater than unity, the natural solution was induced by the thermal effect and the convective cell circulated counterclockwise, as the thermal diffusio n effect prevailed. When the Le number was less than unity, the natural solution was induced by solute effects and the convection cell circulation was clockwise.

The following typical ranges are covered by the numerical results in this study: $0.1 \leq \mathrm{Le} \leq 10$, $10^2 \leq \mathrm{Ra_T} \leq 10^5$, $1 \leq \mathrm{A} \leq 4$ and $\mathrm{Pr} = 7.1$.

4.1 Square Enclosure ($A = 1$)

Above the onset of supercritical convection, Figure 2 to Figure 5 display the streamlines, isotherms and solute iso-concentrations, for $Ra_T = 10^5$ and different Le values. As shown for the two values of Le numbers; 0.1 and 10, the absence of the anti-natural solution is illustrated in Figure 2. For $Le = 1$, as shown in the Figure 4, the natural and anti-natural convective cells are identical but circulating in opposite direction, this result has been also predicted by Mebrouki *et al.,* [46]. As the thermal and solutal diffusivities are equal, the two solutions have the same potential occurrence. For the solution where the cell was counter-clockwise, the convective flow is driven by the thermal effect and by solutal effect when it is in clockwise direction. Owing to this driving effect, the solution led to different rates of thermal and mass exchange. The natural convective solution is defined for the fact it prevailed when initiating the convective flow from a motionless state.

In this regard, when the Le number is bigger than unity, the natural solution is driven by a thermal effect and the convective cell is counter-clockwise, as the thermal diffusivity effect prevailed. When the Le number is smaller than unity, the natural solution is driven by solutal effect and the convective cell circulation was clockwise. On the other hand, the anti-natural solution is obtained by forcing the flow in the opposite direction. Usually, at moderate Le number, the anti-natural solution could be sustained for a significant range of Ra_T. However, it becomes unstable as it approaches the threshold for supercritical convection and a jump to the natural convection solution occurs prematurely.

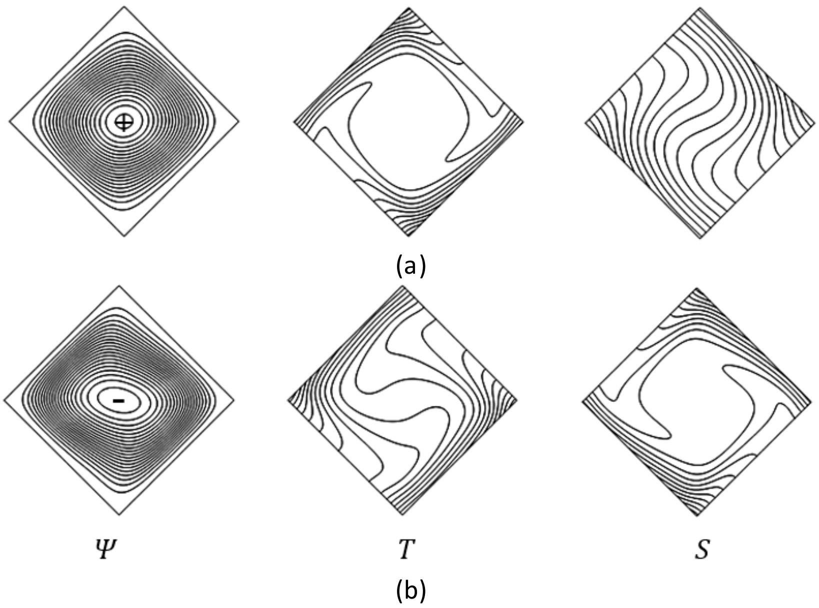

Fig. 2. Ψ, T, and S contours for $Ra_T = 10^5$: (a) $Le = 0.1$, $\Psi_0 = 46.652$, $Nu_m = 5.087$, and $Sh_m = 2.326$; (b) $Le = 10$, $\psi_0 = 11.276$, $Nu_m = 4.056$, and $Sh_m = 8.032$

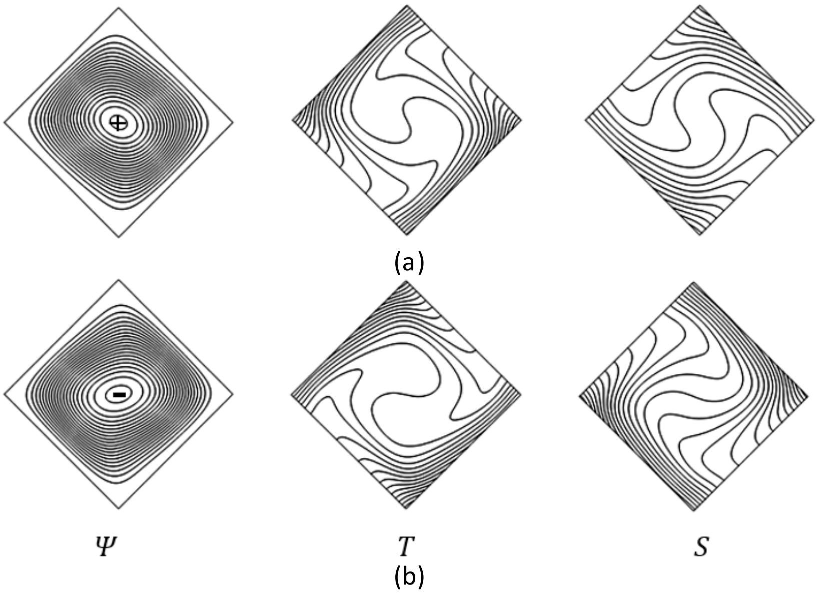

Fig. 3. Ψ, T, and S contours for $Ra_T = 10^5$ and $Le = 0.5$: (a) Ψ_0=20.264, $Nu_m = 4.212$, and $Sh_m = 2.879$; (b) $\Psi_0 = -20.369$, $Nu_m = 3.965$, and $Sh_m = 3.554$

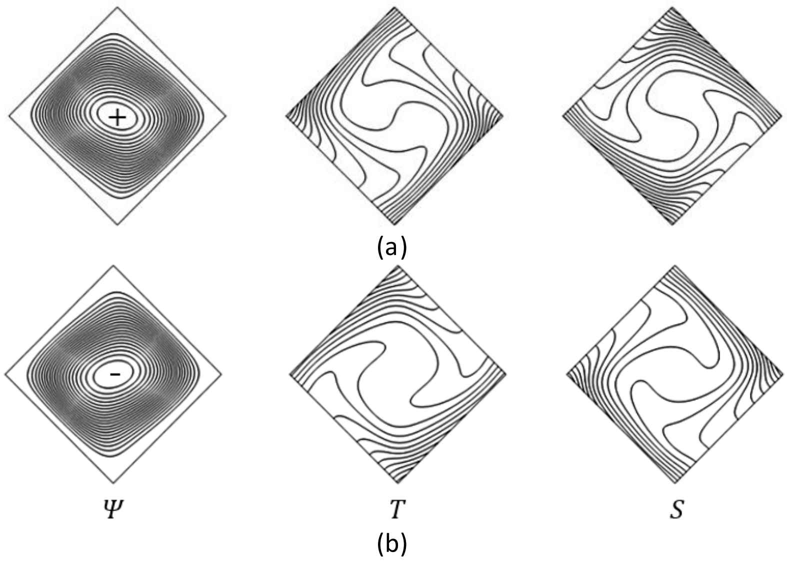

Fig. 4. Ψ, T, and S contours for $Ra_T = 10^5$ and $Le = 1$: (a) $\Psi_0 = 15.767$, $Nu_m = 4.197$ and $Sh_m = 3.574$; (b) $\Psi_0 = -15.767$, $Nu_m = 3.574$ and $Sh_m = 4.197$

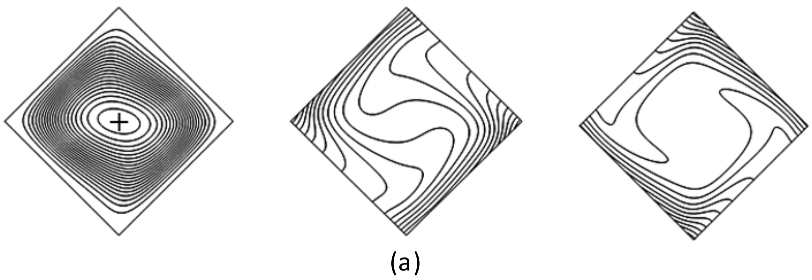

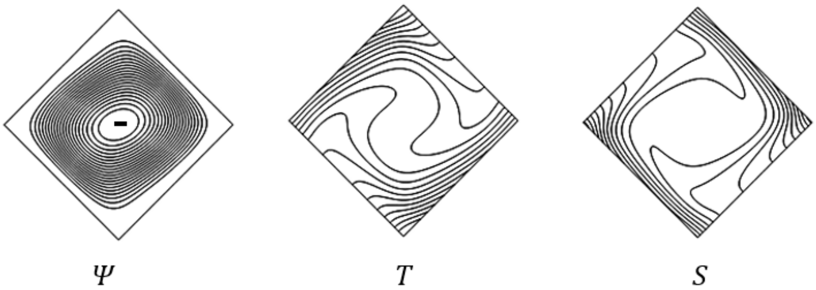

(b)

Fig. 5. Ψ, T, and S contours for $Ra_T = 10^5$ and $Le = 2$: (a) $\Psi_0 = 12.935$, $Nu_m = 4.164$, and $Sh_m = 4.472$; (b) $\Psi_0 = -13.835$, $Nu_m = 3.241$, and $Sh_m = 4.957$

To investigate the convective behavior of the natural and anti-natural solutions, the flow intensity, Ψ_0, and heat and mass transfer rates, Nu_m and Sh_m, are givens in Figure 6 as functions of Ra_T and different values of Le. Regardless the value of Le, both natural and anti-natural solutions showed an increase of Ψ_0, Nu_m and Sh_m with the increasing of Ra_T, a similar trend has been reported by Mebrouki *et al.*, [46].

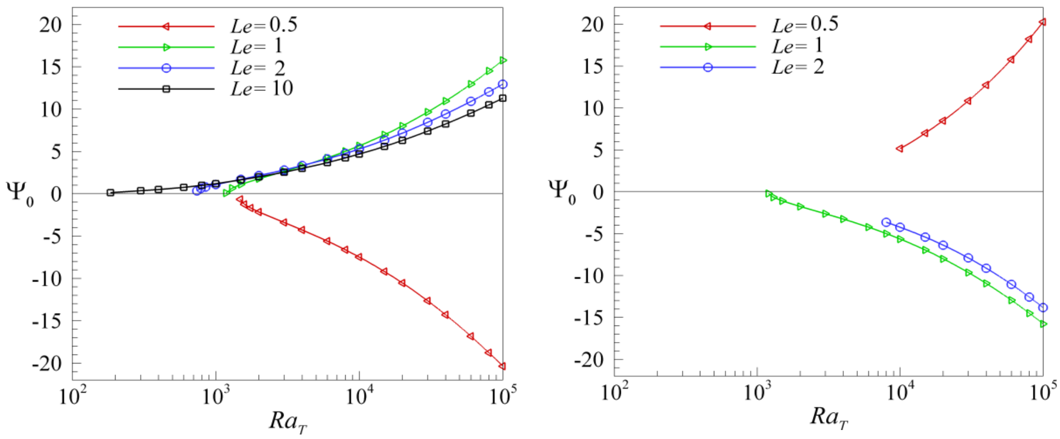

(a)

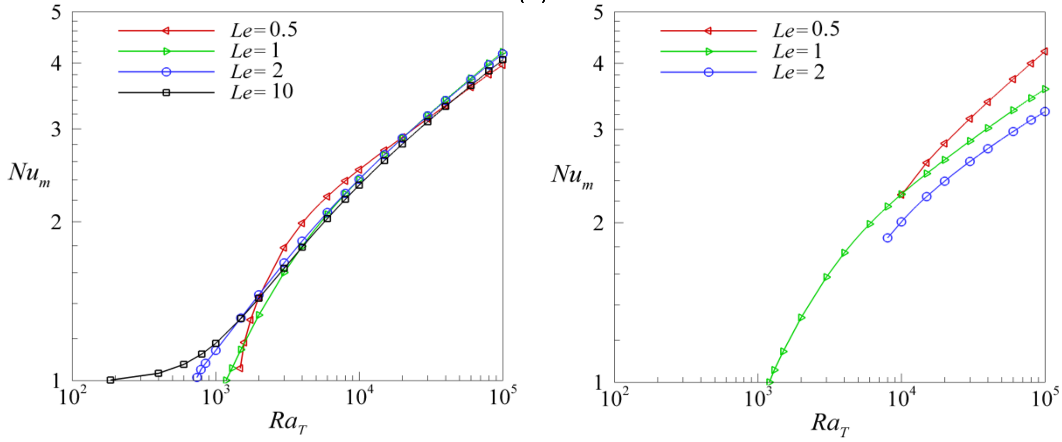

(b)

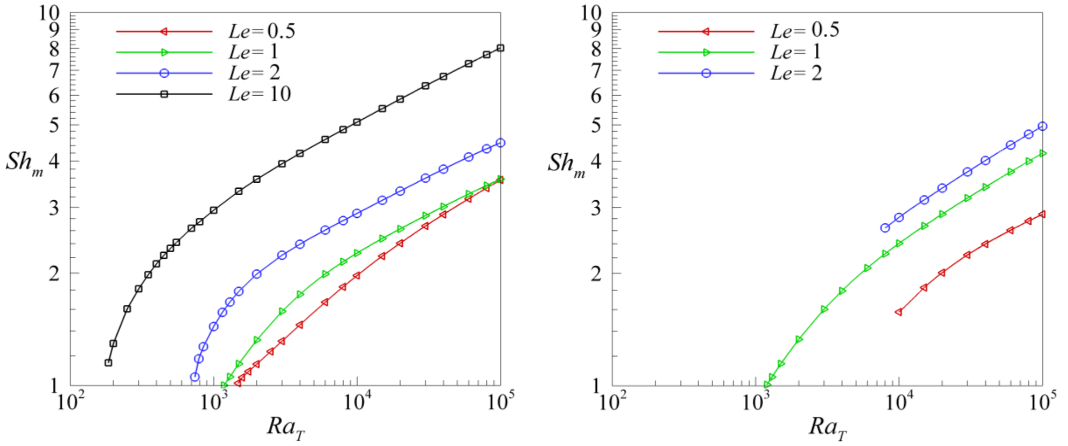

(c)

Fig. 6. Natural (left) and anti-natural (right) solution bifurcation diagrams: (a) flow intensity, Ψ_0; heat and mass transfer rates: (b) Nu_m and (c) Sh_m, as functions of the Ra_T, for various Le values

Concerning, the Le effect, the figure shows that $|\Psi_0|$ decreases and Sh_m increases when Le increases for both natural and anti-natural solutions. However, Nu_m of the anti-natural solution is decreased with the increase of Le. Far from the onset of convection, Nu_m of the natural solution seemed not significantly affected by the Le variation, but near criticality, the threshold of the onset of convection increased with decreasing Le. Consequently, as can be observed from Figure 6, at moderate Le numbers, the anti-natural solution can be maintained over a wide range of Ra numbers. However, it becomes unstable as it approaches the supercritical convection and a jump to the natural convection solution occurs prematurely. As explained earlier, both natural and anti-natural convective solutions bifurcated from the rest state solution at a given critical Ra. The threshold of supercritical convection was obtained accurately using a linear analysis by marching the solution in time for extremely weak convective flows. The flow intensity could be expressed as $\psi_0 = q.e^{pt}$, where q is the amplitude at $t = 0$ (i.e., $\Psi_0 = q$ at $t = 0$). Typically, the value of Ψ_0 within the range of 10^{-6}<Ψ_0<10^{-4} was considered and judged small enough to assume infinitesimal amplitude. When $p < 0$ the flow decaying and when $p > 0$ the flow was amplified. After knowing approximately, the location of the threshold number, using the fully nonlinear solution, the solution is computed for two amounts of Ra; one above and one below the threshold. Above the threshold, the numerical solution marched in time from the rest state solution. However, below the threshold, the solution is initiated with a weak convective flow.

As displayed in Figure 7, the solution is amplified above the threshold and decayed below. The time evolution of the flow intensity is displayed in Figure 7 [46]. A curve fitting using exponential function was performed and the growth rate was computed. For $Le = 1$, the two Rayleigh number values are 1100 and 1250 and the corresponding obtained growth rate are -0.7798 and 0.5640, respectively. The threshold for the onset of convection is obtained when $p = 0$, so by interpolation, it is found that $Ra_{TC}^{sup} = 1187.04$. Redoing the calculations for various Le number, see Table 4, it is found that Ra_{TC}^{sup} obeyed the following relationship with a great accuracy (as predicted in the past by Mebrouki *et al.*, [46]):

$$Ra_{TC}^{sup} = \frac{2374.08}{Le+1} \tag{9}$$

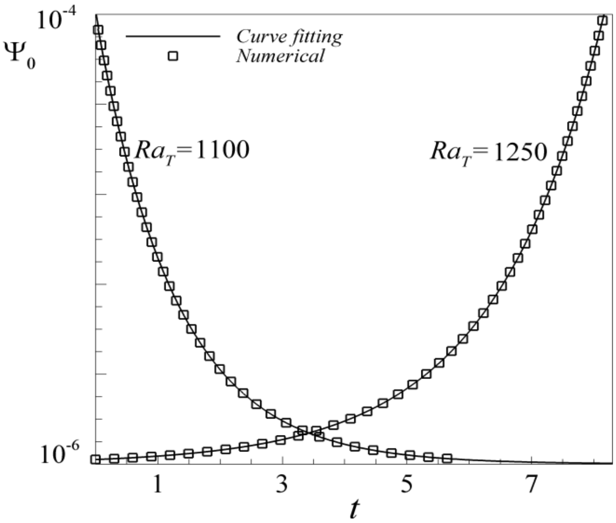

Fig. 7. Natural flow intensity vs. the time for $Le = 1$

Table 4
Computed subcritical and supercritical Ra numbers vs. Le

Le	0.1	0.5	1	2	10
Ra_{TC}^{sup}	2152.5	1581.5	1187.04	789.2	206.5
Ra_{TC}^{sub}	1830	1480	…	740	185

The analytical expression of Ra_{TC}^{sup}, Eq. (9), and the numerical results are depicted in Figure 8 with a very good agreement [46]. The threshold of subcritical convection existed only for the natural convection when $Le \neq 1$, and the values are tabulated in Table 4. The values are obtained by decreasing progressively the Ra number using a small increment until a jump to conductive state occurred. Both the subcritical and supercritical values decreased with increasing Le number. At $Le = 1$, subcritical convection is absent.

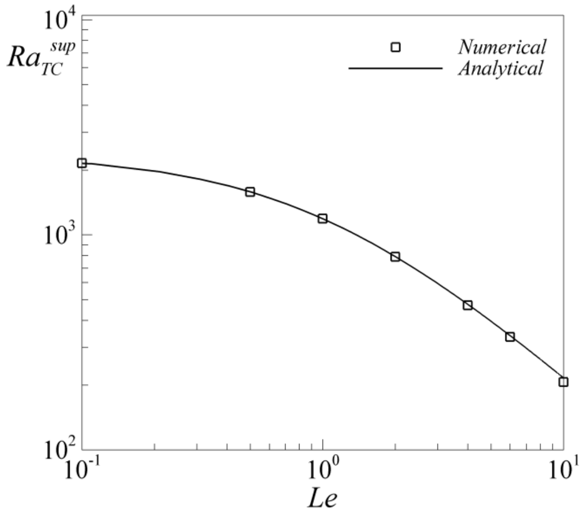

Fig. 8. Supercritical, Ra_{TC}^{sup} vs. Le

Figure 9 displays the bifurcation diagram for $Le = 2$. Below Ra_{TC}^{sub}, the system was unconditionally stable and the solution was characterized by a pure conductive state. Between the critical values, Ra_{TC}^{sub} and Ra_{TC}^{sup}, the convective could be triggered only by a finite amplitude perturbation. The conductive state remained stable to infinitesimal perturbation. Above Ra_{TC}^{sub}, the conductive state became unconditionally instable. Any perturbation, regardless its amplitude, could trigger a convective state. Over stability convection has not been observed in the present investigation.

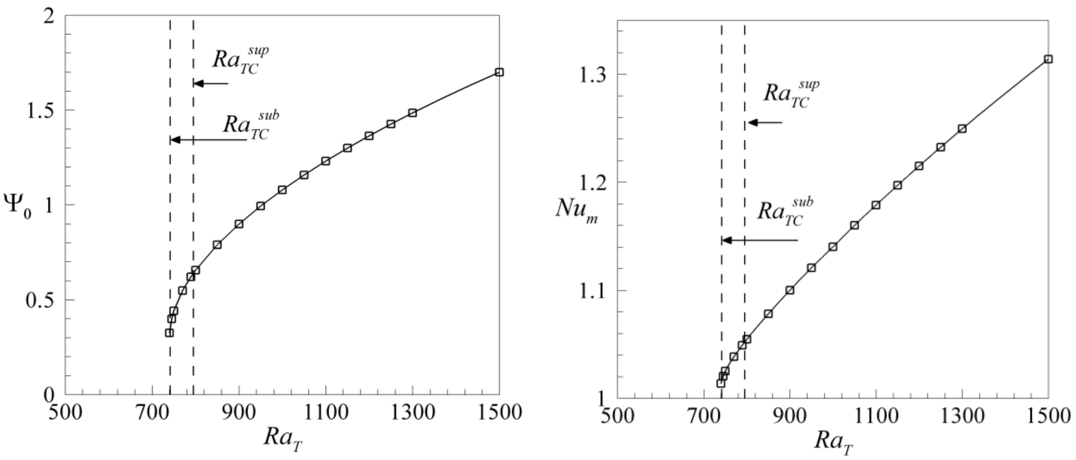

(a) (b)

Fig. 9. *Bifurcation diagram* in terms of (a) intensity of flow [46]; and (b) Nu_m, as function of Ra_T for $Le = 2$

To investigate the convective behavior of the natural and anti-natural solutions, Ψ_0, Nu_m and Sh_m, are givens in Figure 10 as functions of Le and different values of Ra_T. Regardless the value of Le, both natural and anti-natural solutions showed an increase of Ψ_0, Nu_m and Sh_m when Ra_T increases. Concerning, the Lewis effect, the figure shows that the amplitude of the flow for the two natural and anti-natural solutions as well as the heat transfer for the natural solution decrease with increasing Le and subsequently tend towards constant values. However, the mass transfer for the natural and anti-natural solutions increases with Le. Heat transfer for the anti-natural solution increases with Le for Lewis values $Le < 1$ and the inverse for $Le > 1$. The existence of anti-natural solution corresponding to the Ra_T values, $Ra_T = 5.10^3$,10^4 and 10^5, has been found in the following intervals of Le; $0.7 \leq Le \leq 1.73$, $0.5 \leq Le \leq 2.25$ and $0.23 \leq Le \leq 2.89$, respectively. The direction of rotation of the flow is related to the Lewis number value. As shown in Figure 10, the direction of rotation of the flow in the natural solution is clockwise ($\Psi_0 < 0$) when $Le < 1.0$, and trigonometric ($\Psi_0 > 0$) when $Le \geq 1.0$. To explain the direction of rotation of the flow, one takes the case of the natural solution with the value of the thermal Rayleigh number $\mathrm{Ra_T} = 10^4$. Consider the case of $Le > 1$, in this situation, the thermal diffusivity, α, is greater than the mass diffusivity, D, therefore, the natural solution is induced by the thermal effect and the convective cell circulates in counterclockwise. In this situation, the quantity of the mass transported by convection along the walls where the mass flow is imposed and is greater than that of the heat transported along the walls where the heat flow is imposed.

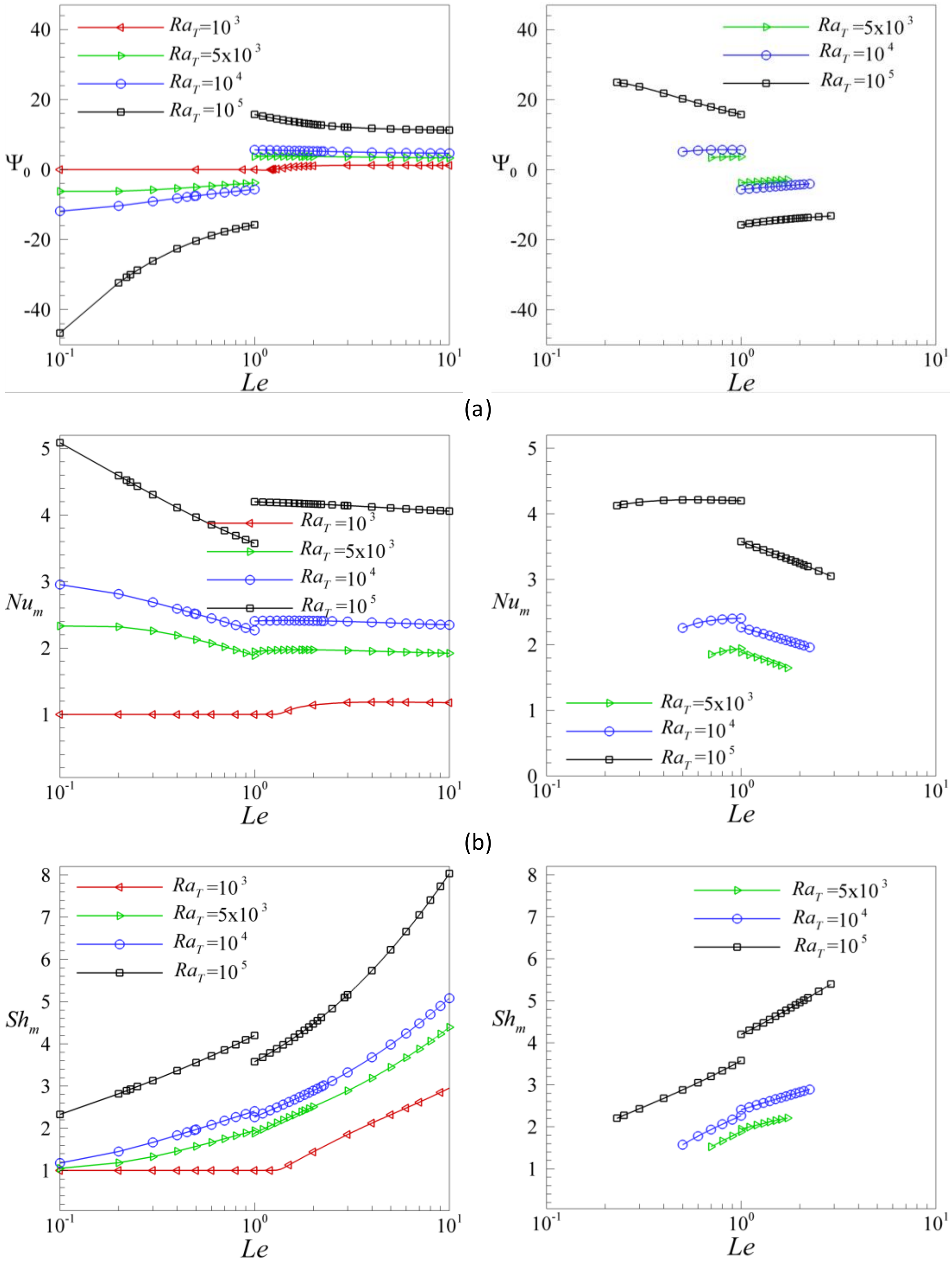

(c)

Fig. 10. Natural (left) and anti-natural (right) solution bifurcation diagrams: (a) Ψ_0; (b) Nu_m; (c) Sh_m, vs. Le and for various Ra_T

This is clarified by the numerical results which are expressed by the average Sherwood and Nusselt numbers corresponding to the value of $Le = 1.14$ ($\mathrm{Sh_m} = 2.61$ and $\mathrm{Nu_m} = 2.14$). In the case of $Le < 1$, the natural solution is induced by the mass effect and the convective cell circulates in a clockwise direction, and the amount of heat transported by the convection along the walls where the heat flow is imposed is greater than that of the mass transported along the walls where the mass flow is imposed.

As an example, the Nu_m and Sh_m numbers are $Nu_m = 2.34$ and $Sh_m = 2.26$ for $Le = 0.8$. The convective cell of the anti-natural solution circulates clockwise for $Le > 1$, and counterclockwise for

$Le < 1$. We observe that for the value of $Le = 1$, the convective cell of the natural solution circulates in an anti-clockwise direction, and that of the antinatural solution circulates in the opposite direction. The quantity of heat transported by natural convection expressed by the Nusselt number ($Nu_m = 2.26$), is equal to the quantity of mass transported by antinatural convection expressed by the mean Sherwood number ($Sh_m = 2.26$). The quantity of mass transported by natural convection expressed by the average Sherwood number ($Sh_m = 2.40$), is equal to the quantity of heat transported by the antinatural convection expressed by the average Nusselt number ($Nu_m = 2.40$). As it is presented in the figures below for $Ra_T = 10^3$ we notice the existence of only one solution and the heat and mass transfer are purely diffusive ($Nu_m = S_m = 1$) for the low values of Le ($Le < 2$), thereafter the mass transfer increases with the increase of Le, and the heat transfer tends towards a constant value from $Le = 3$. The flow intensity is low for this value of Ra_T.

4.2 Slender Cavity (A = 4)

The flow intensity, Ψ_0, as well as the thermal exchange rate, Nu_m, vs. Ra_T are shown in Figure 11. In general, the strength of convection (Ψ_0) and thermal exchange rate (Nu_m) increase as the Rayleigh number, Ra_T, augments, for the different amounts of Le. Regarding the Lewis effect, the figure shows that near the threshold, Ψ_0 increases as Le increases and the reverse occurs far from the convection threshold. However, far from the convection threshold, Nu_m does not appear to be significantly affected by the variation of Le, but near the threshold, the convection increases with increasing Le.

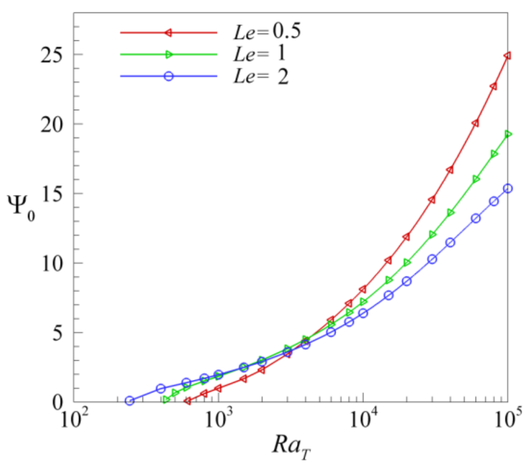

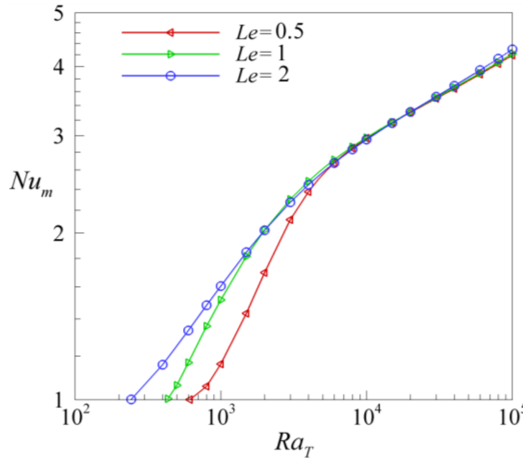

Fig. 11. (a) Flow intensity; (b) heat transfer rate, as function of the Ra_T for various Le values with A = 4

Table 5 presents the supercritical Rayleigh number, Ra_{TC}^{sup} for $A = 4$ and various Le. These results show that the convection in this case; i.e., for $A = 4$, is triggered for the supercritical Ra smaller than for the case of a square cavity, $A = 1$.

Table 5
Variation of the supercritical Ra number for $A = 4$ and different Le values

Le	0.5	1	2
Ra_{TC}^{sup}	614.4183	433.8472	242.9157

Figure 12 shows the streamlines, isotherms and iso-concentrations obtained for $Ra_T = 10^4$ and different values of Le. For $Le = 0.1$, the flow circulation is clockwise. When $Le > 1$, the circulation of the convection cell is counterclockwise.

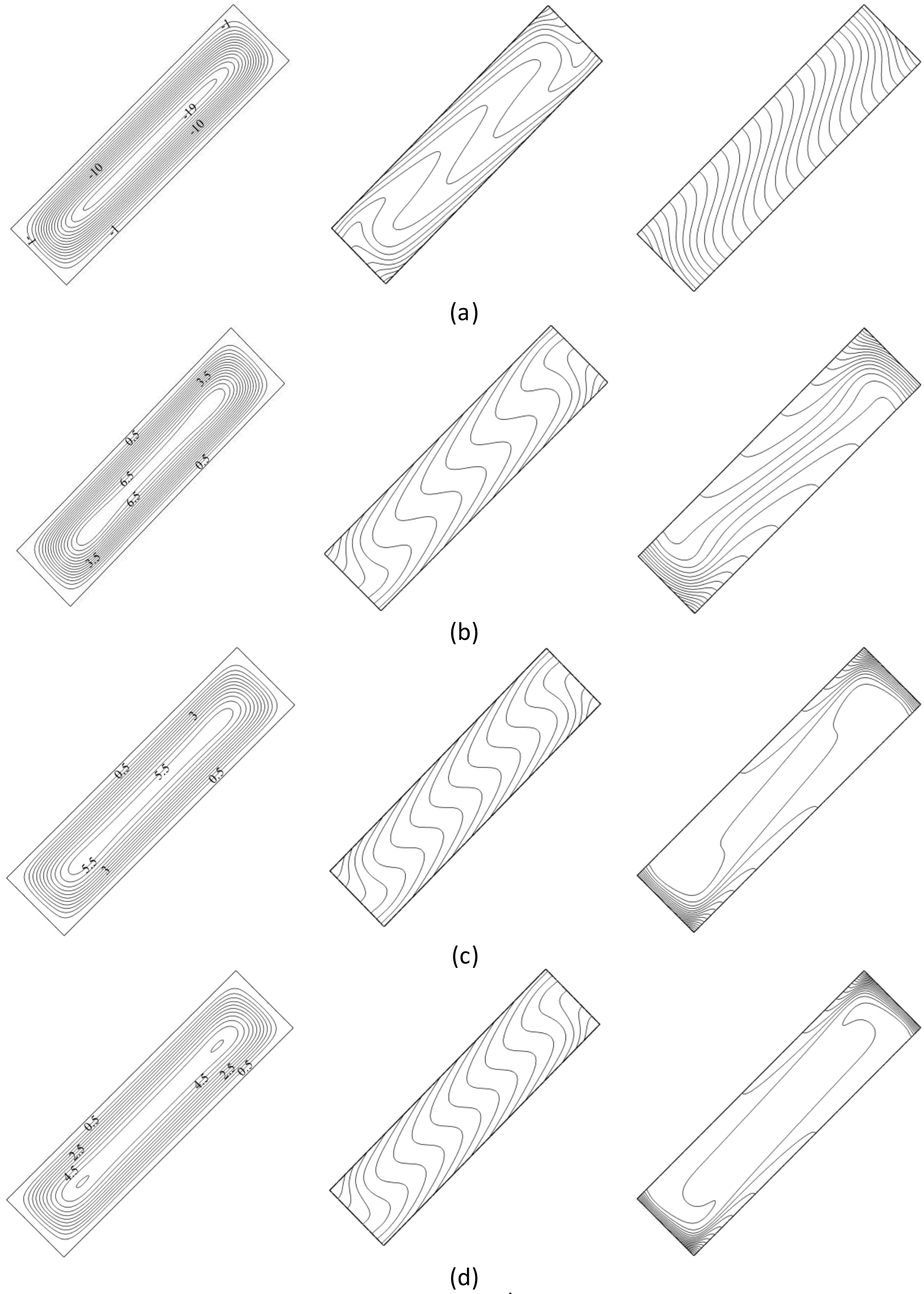

Fig. 12. Ψ, T and S contours for $Ra_T = 10^4$: (a) $Le = 0.1$, $\Psi_0 = -19.500$, $Nu_m = 3.278$ and $Sh_m = 0.488$; (b) $Le = 1$, $\Psi_0 = 7.207$, $Nu_m = 2.975$ and $Sh_m = 1.550$; (c) $Le = 5$, $\Psi_0 = 5.697$, $Nu_m = 2.916$ and $Sh_m = 3.196$; (d) $Le = 10$, $\Psi_0 = 5.386$, $Nu_m = 2.899$ and $Sh_m = 4.161$

This is visible just when we compare the isotherms and iso-concentrations of Figure 12(a), and those of Figure 12(b). The amplitude of flow and thermal exchange decrease with increasing Le. However, mass transfer increases with Le.

Taking the solution of the pure conduction as initial conditions, temporal evolution of stream function at the enclosure center and the stream function contours are shown in Figure 13 for an aspect ratio $A = 4$, $Ra_T = 800\ to\ 10^4$, $Pr = 10$, $Le = 1$ and $N = 1$. It is found that an oscillatory flow occurs within the limit of the thermal Rayleigh number $Ra_T = 925 - 1135$. Outside this interval, the convective solution converges to a stable solution and the structure of the flow is unicellular.

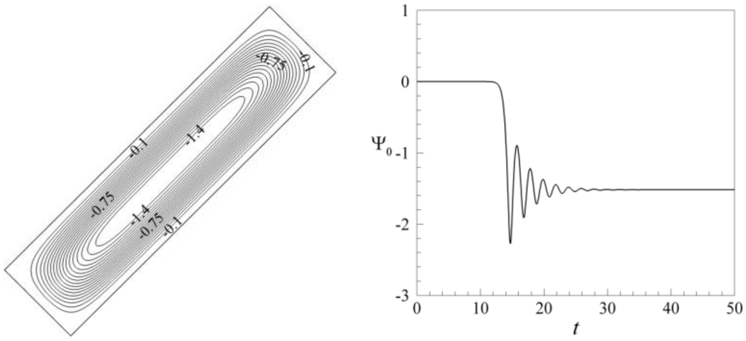

(a)

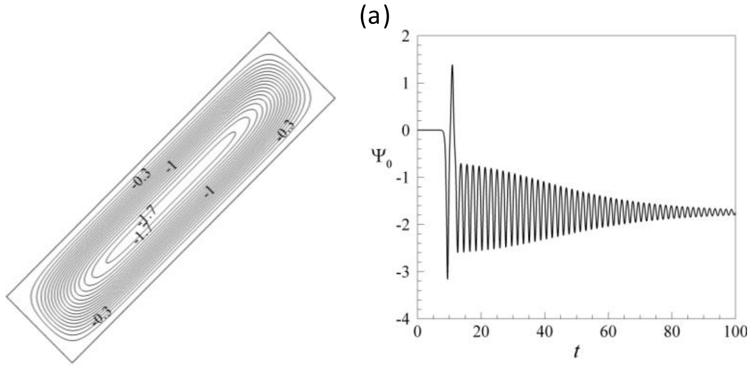

(b)

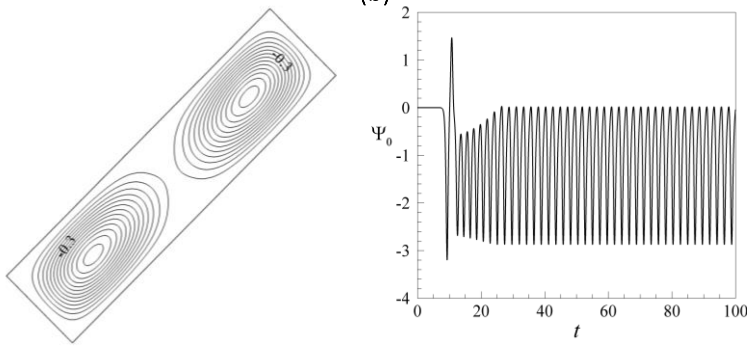

(c)

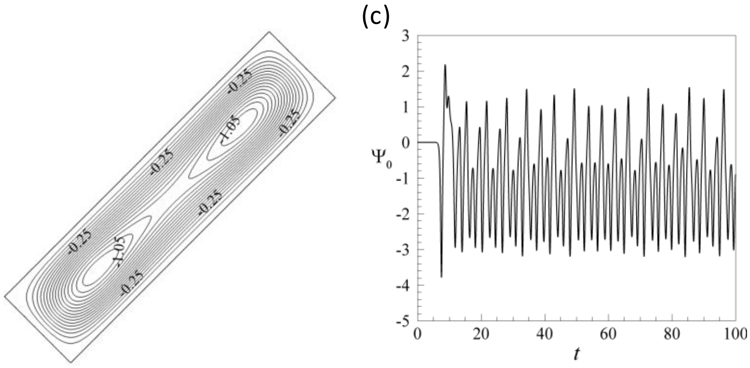

(d)

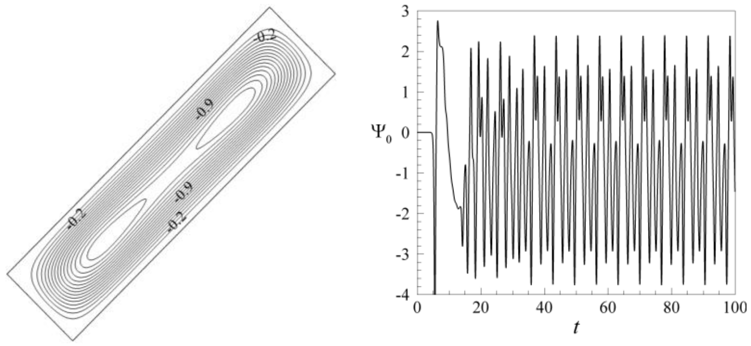

(e)

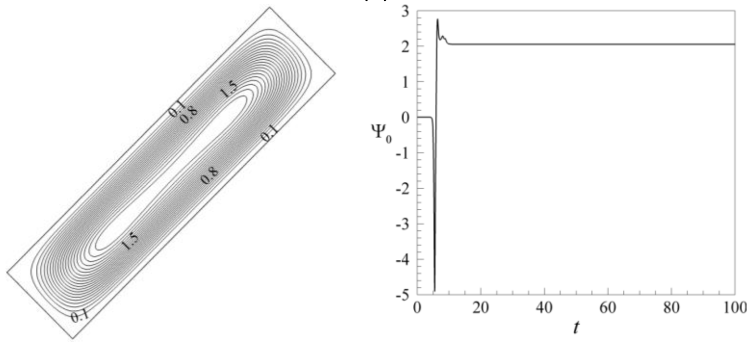

(f)

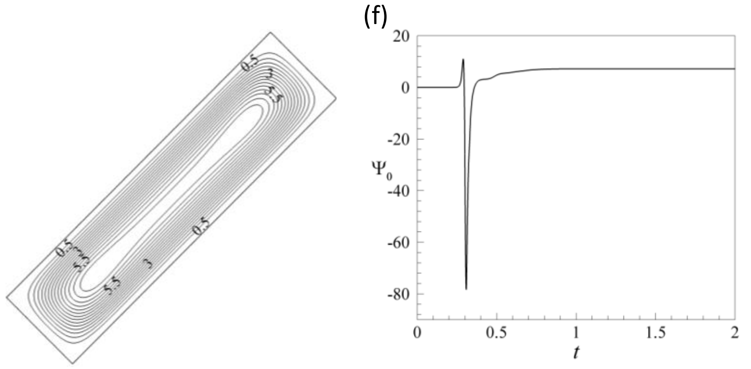

(g)

Fig. 13. Ψ contours (left), temporal evolution of Ψ in the cavity center (right): (a) $Ra_T = 800$; (b) $Ra_T = 920$; (c) $Ra_T = 925$; (d) $Ra_T = 10^3$; (e) $Ra_T = 1135$; (f) $Ra_T = 1140$; (g) $Ra_T = 10^4$

Figure 14 shows the oscillatory convective solution of the stream function over time between $t = 14.6$ and $t = 16$, for a constant value of the thermal Ra number $Ra_T = 10^3$;. Two main types of flow structure are observed; a flow composed of three contra-rotating convection cells, where the value of the intensity of the flow at the enclosure center is positive $\Psi_0 > 0$, and a single-cell flow where $\Psi_0 < 0$ (Figure 14). The other structure composed of two cells is an intermediate structure during the creation of the multicellular structure of the monocellular structure as shown in Figure 15, between $t = 14.8$ and $t = 15$. Also, during the inverse change of the multicellular structure to the mono-cellular structure Figure 15, between $t = 15.6$ and $t = 15.8$.

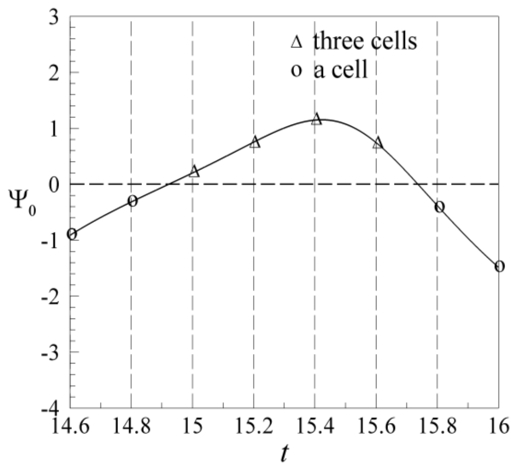

Fig. 14. Variation of Ψ with t in the cavity center for $Ra_T = 10^3$

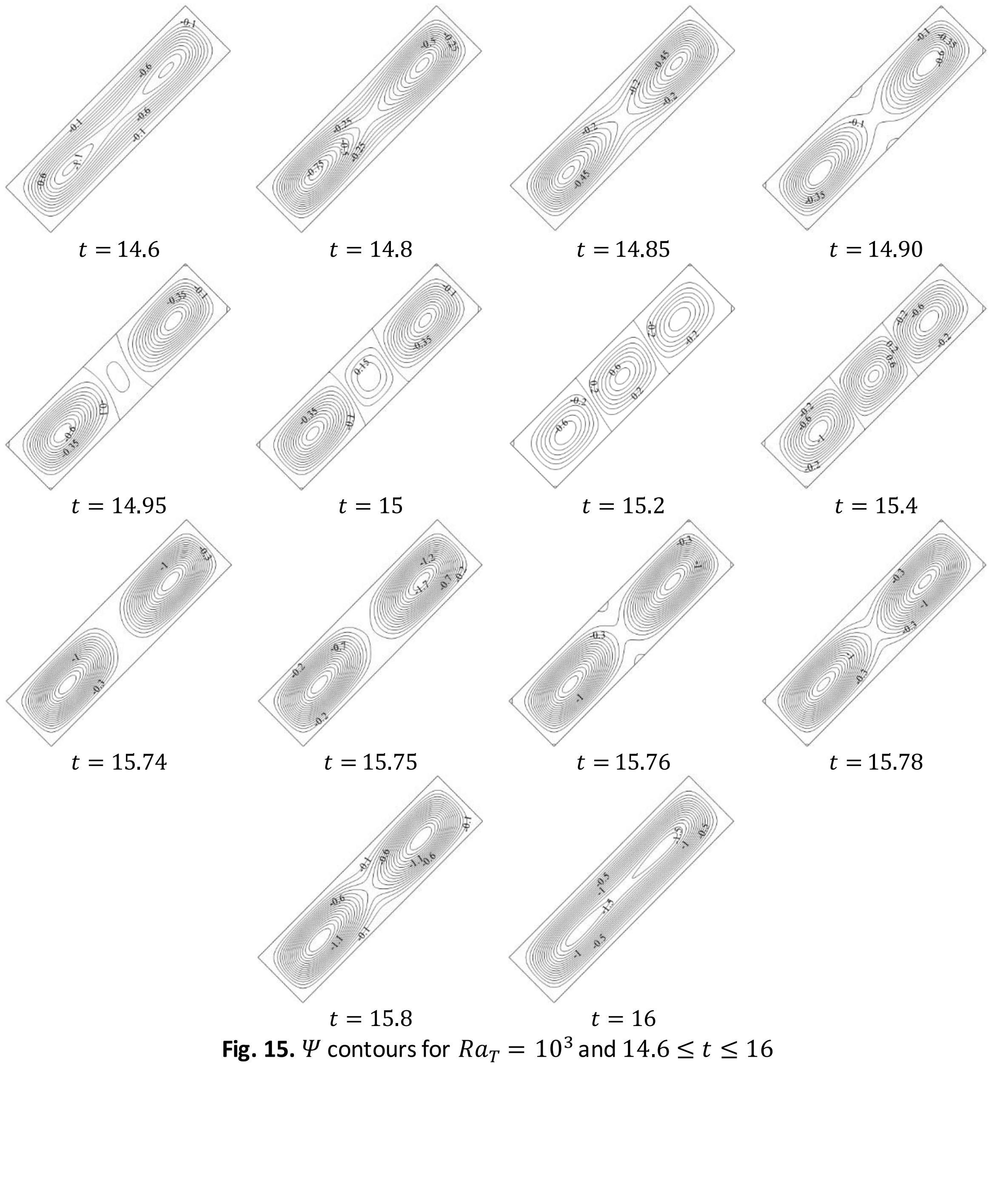

Fig. 15. Ψ contours for $Ra_T = 10^3$ and $14.6 \leq t \leq 16$

5. Conclusions

In a square enclosure, thermosolutal convection was studied numerically. The circumstance where the enclosure was slanted 45 degrees and the buoyancy ratio was one ($N = 1$) was taken into consideration. The convective flow is governed by a different control parameter, namely Ra_T, Pr, Le, A, and Φ, of the cavity regarding the horizontal plane. The outcomes are shown in terms of Nu_m, Sh_m, and intensity of flow as functions of Ra_T and Le numbers. The main conclusion of the present analysis are as follows:

(i) The co-existence of natural and anti-natural convective solutions was demonstrated.
(ii) The Le number determined the criteria for the beginning of supercritical and subcritical convection.
(iii) The flow intensity and the thermal and mass exchange rates increased with increasing the Rayleigh number, Ra_T.
(iv) As the Le number increased, the flow intensity decreased and the masse exchange rate rose.
(v) For an infinity layer, the convection is triggered for smaller thermal Rayleigh numbers than for a square cavity.
(vi) For an $aspect\ ratio$ of 4, different flow patterns were observed and the interval of existence of an oscillatory solution was determined.
(vii) It must be noted that the results in this research only applied to the scenario where the buoyancy ratio was equal to 1. However, in the case of helping and opposing flows, where buoyancy forces are friendly, the current hypothesis might also be applicable.
(viii) In practice, fluids are not always Newtonian; to deepen knowledge in this area it would be interesting to repeat the same study for a non-Newtonian fluid.

References

[1] Lapwood, E. R. "Convection of a fluid in a porous medium." In *Mathematical Proceedings of the Cambridge Philosophical Society*, vol. 44, no. 4, pp. 508-521. Cambridge University Press, 1948. https://doi.org/10.1017/S030500410002452X

[2] Davis, G. de Vahl. "Natural convection of air in a square cavity: a bench mark numerical solution." *International Journal for Numerical Methods in Fluids* 3, no. 3 (1983): 249-264. https://doi.org/10.1002/fld.1650030305

[3] Kimura, S., M. Vynnycky, and F. Alavyoon. "Unicellular natural circulation in a shallow horizontal porous layer heated from below by a constant flux." *Journal of Fluid Mechanics* 294 (1995): 231-257. https://doi.org/10.1017/S0022112095002874

[4] Al-Azawy, Mohammed Ghalib, Saleem Khalefa Kadhim, and Azzam Sabah Hameed. "Newtonian and non-newtonian blood rheology inside a model of stenosis." *CFD Letters* 12, no. 11 (2020): 27-36. https://doi.org/10.37934/cfdl.12.11.2736

[5] Mojtabi, Abdelkader, and Marie-Catherine Charrier-Mojtabi. "Double-diffusive convection in porous media." In *Handbook of Porous Media*, pp. 287-338. CRC Press, 2005. https://doi.org/10.1201/9780415876384-10

[6] Nishimura, Tatsuo, Mikio Wakamatsu, and Alexandru M. Morega. "Oscillatory double-diffusive convection in a rectangular enclosure with combined horizontal temperature and concentration gradients." *International Journal of Heat and Mass Transfer* 41, no. 11 (1998): 1601-1611. https://doi.org/10.1016/S0017-9310(97)00271-8

[7] Weaver, J. A., and Raymond Viskanta. "Natural convection in binary gases driven by combined horizontal thermal and vertical solutal gradients." *Experimental Thermal and Fluid Science* 5, no. 1 (1992): 57-68. https://doi.org/10.1016/0894-1777(92)90056-B

[8] Chamkha, Ali J., and Hameed Al-Naser. "Double-diffusive convection in an inclined porous enclosure with opposing temperature and concentration gradients." *International Journal of Thermal Sciences* 40, no. 3 (2001): 227-244. https://doi.org/10.1016/S1290-0729(00)01213-8

[9] Mohamad, Abdulmajeed A., and Rachid Bennacer. "Natural convection in a confined saturated porous medium with horizontal temperature and vertical solutal gradients." *International Journal of Thermal Sciences* 40, no. 1 (2001): 82-93. https://doi.org/10.1016/S1290-0729(00)01182-0

[10] Mohamad, A. A., and R. Bennacer. "Double diffusion, natural convection in an enclosure filled with saturated porous medium subjected to cross gradients; stably stratified fluid." *International Journal of Heat and Mass Transfer* 45, no. 18 (2002): 3725-3740. https://doi.org/10.1016/S0017-9310(02)00093-5

[11] Benhadji, K., and P. Vasseur. "Double diffusive convection in a shallow porous cavity filled with a non-Newtonian fluid." *International Communications in Heat and Mass Transfer* 28, no. 6 (2001): 763-772. https://doi.org/10.1016/S0735-1933(01)00280-9

[12] Bahloul, A., N. Boutana, and P. Vasseur. "Double-diffusive and Soret-induced convection in a shallow horizontal porous layer." *Journal of Fluid Mechanics* 491 (2003): 325-352. https://doi.org/10.1017/S0022112003005524

[13] Bahloul, A., P. Vasseur, and L. Robillard. "Convection of a binary fluid saturating a shallow porous cavity subjected to cross heat fluxes." *Journal of Fluid Mechanics* 574 (2007): 317-342. https://doi.org/10.1017/S0022112006004113

[14] Rebhi, Redha, Mahmoud Mamou, Patrick Vasseur, and Mounir Alliche. "Form drag effect on the onset of non-linear convection and Hopf bifurcation in binary fluid saturating a tall porous cavity." *International Journal of Heat and Mass Transfer* 100 (2016): 178-190. https://doi.org/10.1016/j.ijheatmasstransfer.2016.04.060

[15] Kumar, Gautam, Puranam Anantha Lakshmi Narayana, and Kirti Chandra Sahu. "Linear and nonlinear thermosolutal instabilities in an inclined porous layer." *Proceedings of the Royal Society A* 476, no. 2233 (2020): 20190705. https://doi.org/10.1098/rspa.2019.0705

[16] Saxena, Ashish, Vimal Kishor, Suneet Singh, and Atul Srivastava. "Experimental and numerical study on the onset of natural convection in a cavity open at the top." *Physics of Fluids* 30, no. 5 (2018): 057102. https://doi.org/10.1063/1.5025092

[17] Bihiche, K., M. Lamsaadi, and M. Hasnaoui. "Multiple steady state solutions for double-diffusive convection in a shallow horizontal rectangular cavity uniformly heated and salted from the side and filled with non-Newtonian power-law fluids." *Journal of Non-Newtonian Fluid Mechanics* 283 (2020): 104349. https://doi.org/10.1016/j.jnnfm.2020.104349

[18] Bourich, M., M. Hasnaoui, and A. Amahmid. "A scale analysis of thermosolutal convection in a saturated porous enclosure submitted to vertical temperature and horizontal concentration gradients." *Energy Conversion and Management* 45, no. 18-19 (2004): 2795-2811. https://doi.org/10.1016/j.enconman.2004.01.010

[19] Bahloul, A., L. Kalla, R. Bennacer, H. Beji, and P. Vasseur. "Natural convection in a vertical porous slot heated from below and with horizontal concentration gradients." *International Journal of Thermal Sciences* 43, no. 7 (2004): 653-663. https://doi.org/10.1016/j.ijthermalsci.2003.10.012

[20] Bourich, M., M. Hasnaoui, and A. Amahmid. "Double-diffusive natural convection in a porous enclosure partially heated from below and differentially salted." *International Journal of Heat and Fluid Flow* 25, no. 6 (2004): 1034-1046. https://doi.org/10.1016/j.ijheatfluidflow.2004.01.003

[21] Kramer, Janja, Renata Jecl, and L. Skerget. *Natural convection in porous media under cross temperature and concentration gradients with Boundary Element Method*. Vol. 47. WIT Press, 2008. https://doi.org/10.2495/BE080071

[22] Chamkha, Ali J., Ali Al-Mudhaf, and Eisa Al-Meshaiei. "Thermo-solutal convection in an inclined porous cavity with various aspect ratios under mixed thermal and species boundary conditions." *Heat Transfer-Asian Research* 40, no. 8 (2011): 693-720. https://doi.org/10.1002/htj.20369

[23] Balla, Chandra Shekar, and Kishan Naikoti. "Soret and Dufour effects on free convective heat and solute transfer in fluid saturated inclined porous cavity." *Engineering Science and Technology, an International Journal* 18, no. 4 (2015): 543-554. https://doi.org/10.1016/j.jestch.2015.04.001

[24] Ouzaouit, Meriem, Btissam Abourida, Lahoucine Belarche, Hicham Doghmi, and Mohamed Sannad. "Numerical study of the thermosolutal convection in a 3-D cavity submitted to cross gradients of temperature and concentration." *Thermal Science* 23, no. 3 Part B (2019): 1923-1933. https://doi.org/10.2298/TSCI170809070O

[25] Balla, Chandra Shekar, Naikoti Kishan, Rama SR Gorla, and B. J. Gireesha. "MHD boundary layer flow and heat transfer in an inclined porous square cavity filled with nanofluids." *Ain Shams Engineering Journal* 8, no. 2 (2017): 237-254. https://doi.org/10.1016/j.asej.2016.02.010

[26] Balla, Chandra Shekar, C. Haritha, and Naikoti Kishan. "Magnetohydrodynamic convection in a porous square cavity filled by a nanofluid with viscous dissipation effects." *Proceedings of the Institution of Mechanical Engineers, Part E: Journal of Process Mechanical Engineering* 233, no. 3 (2019): 474-488. https://doi.org/10.1177/0954408918765314

[27] Chakkingal, Manu, Roland Voigt, Chris R. Kleijn, and Saša Kenjereš. "Effect of double-diffusive convection with cross gradients on heat and mass transfer in a cubical enclosure with adiabatic cylindrical obstacles." *International Journal of Heat and Fluid Flow* 83 (2020): 108574. https://doi.org/10.1016/j.ijheatfluidflow.2020.108574

[28] Rebhi, Redha, Noureddine Hadidi, and Rachid Bennacer. "Non-Darcian effect on double-diffusive natural convection inside an inclined square Dupuit-Darcy porous cavity under a magnetic field." *Thermal Science* 25, no. 1 Part A (2021): 121-132. https://doi.org/10.2298/TSCI190117271R
[29] Ouazaa, Nabil, Smail Benisaad, and Mahmoud Mamou. "Double diffusion convection in a tilted square porous domain under cross temperature and concentration gradients." *U.P.B. Scientific Bulletin, Series D* 82, no. 2 (2020): 131-142.
[30] Ghiasi, Emran Khoshrouye, and Reza Saleh. "Analytical and numerical solutions to the 2D Sakiadis flow of Casson fluid with cross diffusion, inclined magnetic force, viscous dissipation and thermal radiation based on Buongiorno's mathematical model." *CFD Letters* 11, no. 1 (2019): 40-54.
[31] Khdher, Abdolbaqi Mohammed, Nor Azwadi Che Sidik, Siti Nurul Akmal Yusof, and M'hamed Beriache. "Heat Transfer Enhancement in Straight Channel with Nanofluid In Fully Developed Turbulent Flow." *Journal of Advanced Research in Applied Mechanics* 63, no. 1 (2019): 1-15.
[32] Khan, Ansab Azam, Khairy Zaimi, Suliadi Firdaus Sufahani, and Mohammad Ferdows. "MHD flow and heat transfer of double stratified micropolar fluid over a vertical permeable shrinking/stretching sheet with chemical reaction and heat source." *Journal of Advanced Research in Applied Sciences and Engineering Technology* 21, no. 1 (2020): 1-14. https://doi.org/10.37934/araset.21.1.114
[33] Yusof, Nur Syamila, Siti Khuzaimah Soid, Mohd Rijal Illias, Ahmad Sukri Abd Aziz, and Nor Ain Azeany Mohd Nasir. "Radiative Boundary Layer Flow of Casson Fluid Over an Exponentially Permeable Slippery Riga Plate with Viscous Dissipation." *Journal of Advanced Research in Applied Sciences and Engineering Technology* 21, no. 1 (2020): 41-51. https://doi.org/10.37934/araset.21.1.4151
[34] Wahid, Nur Syahirah, Mohd Ezad Hafidz Hafidzuddin, Norihan Md Arifin, Mustafa Turkyilmazoglu, and Nor Aliza Abd Rahmin. "Magnetohydrodynamic (MHD) slip darcy flow of viscoelastic fluid over a stretching sheet and heat transfer with thermal radiation and viscous dissipation." *CFD Letters* 12, no. 1 (2020): 1-12.
[35] Mahrous, Samar A., Nor Azwadi Che Sidik, and Khalid M. Saqr. "Newtonian and non-Newtonian CFD models of intracranial aneurysm: a review." *CFD Letters* 12, no. 1 (2020): 62-86.
[36] Parvin, Shahanaz, Siti Suzilliana Putri Mohamed Isa, Norihan Md Arifin, and Fadzilah Md Ali. "The Magnetohydrodynamics Casson Fluid Flow, Heat and Mass Transfer Due to the Presence of Assisting Flow and Buoyancy Ratio Parameters." *CFD Letters* 12, no. 8 (2020): 64-75. https://doi.org/10.37934/cfdl.12.8.6475
[37] Sikdar, Prabir, and Sunil Manohar Dash. "A Numerical Study on the Lid-Driven Cavity with Power-Law Fluids at Different Moving Lengths of the Top Lid." *CFD Letters* 12, no. 6 (2020): 107-117. https://doi.org/10.37934/cfdl.12.6.107117
[38] Paliwal, R. C., and C. F. Chen. "Double-diffusive instability in an inclined fluid layer. Part 1. Experimental investigation." *Journal of Fluid Mechanics* 98, no. 4 (1980): 755-768. https://doi.org/10.1017/S0022112080000377
[39] Paliwal, R. C., and C. F. Chen. "Double-diffusive instability in an inclined fluid layer Part 2. Stability analysis." *Journal of Fluid Mechanics* 98, no. 4 (1980): 769-785. https://doi.org/10.1017/S0022112080000389
[40] Bodduna, Jamuna, M. P. Mallesh, Chandra Shekar Balla, and Sabir Ali Shehzad. "Activation energy process in bioconvection nanofluid flow through porous cavity." *Journal of Porous Media* 25, no. 4 (2022): 37-51. https://doi.org/10.1615/JPorMedia.2022040230
[41] Akram, Safia, Maria Athar, Khalid Saeed, and Mir Yasir Umair. "Nanomaterials effects on induced magnetic field and double-diffusivity convection on peristaltic transport of Prandtl nanofluids in inclined asymmetric channel." *Nanomaterials and Nanotechnology* 12 (2022): 18479804211048630. https://doi.org/10.1177/18479804211048630
[42] Saeed, Khalid, Safia Akram, Adeel Ahmad, Maria Athar, Muhammad Imran, and Taseer Muhammad. "Impact of partial slip on double diffusion convection and inclined magnetic field on peristaltic wave of six-constant Jeffreys nanofluid along asymmetric channel." *The European Physical Journal Plus* 137, no. 3 (2022): 364. https://doi.org/10.1140/epjp/s13360-022-02553-6
[43] Akram, Safia, Alia Razia, Mir Yasir Umair, Tuqa Abdulrazzaq, and Raad Z. Homod. "Double-diffusive convection on peristaltic flow of hyperbolic tangent nanofluid in non-uniform channel with induced magnetic field." *Mathematical Methods in the Applied Sciences* (2022). https://doi.org/10.1002/mma.8188
[44] Phu, Nguyen Minh, and Pham Ba Thao. "Thermohydraulic performance of a fin and inclined flat tube heat exchanger: A numerical analysis." *CFD Letters* 13, no. 7 (2021): 1-12. https://doi.org/10.37934/cfdl.13.7.112
[45] Lounis, Selma, Redha Rebhi, Noureddine Hadidi, Giulio Lorenzini, Younes Menni, Houari Ameur, and Nor Azwadi Che Sidik. "Thermo-Solutal Convection of Carreau-Yasuda Non-Newtonian Fluids in Inclined Square Cavities Under Dufour and Soret Impacts." *CFD Letters* 14, no. 3 (2022): 96-118. https://doi.org/10.37934/cfdl.14.3.96118
[46] Mebrouki, A., Mahmoud Mamou, and Rachid Saim. "Thermosolutal convection in a tilted square fluid enclosure subject to cross fluxes of heat and solute." *16èmes Journées Internationales de Thermique (JITH 2013)* (2013).

[47] Mamou, M., P. Vasseur, and E. Bilgen. "Analytical and numerical study of double diffusive convection in a vertical enclosure." *Heat and Mass Transfer* 32, no. 1 (1996): 115-125. https://doi.org/10.1007/s002310050100

[48] Lee, Jin Wook, and Jae Min Hyun. "Double diffusive convection in a cavity under a vertical solutal gradient and a horizontal temperature gradient." *International Journal of Heat and Mass Transfer* 34, no. 9 (1991): 2423-2427. https://doi.org/10.1016/0017-9310(91)90066-N